Electron. Mater. Lett., Vol. 11, No. 2 (2015), pp. 225-231
DOI: 10.1007/s13391-014-4265-5

Dielectric Spectroscopy of High Aspect Ratio Graphene-Polyurethane Nanocomposites

Rahim Jan,* Amir Habib, Hina Abbassi, and Shahid Amir

School of Chemical & Materials Engineering (SCME), National University of Sciences & Technology (NUST), H-12 Campus, Islamabad, 44000, Pakistan

(received date: 30 August 2014 / accepted date: 30 October 2014 / published date: 10 March 2015)

High aspect ratio graphene nanosheets (GNS), prepared via liquid exfoliation, are homogeneously dispersed in thermoplastic polyurethane (TPU). Dielectric spectroscopy results are reported for these nanocomposites (up to 0.55 vol. % GNS) in the frequency range of 100 Hz to 5 MHz. The as-prepared GNS increased the AC conductivity 10 - 1000 times across the given frequency range. The dielectric constant is increased 5 - 6 times at 100 Hz for the maximum loading of GNS when compared with the pristine TPU, with subsequently high dielectric loss making them a suitable candidate for high energy dissipation applications such as EMI shielding. The temperature effects on the dielectric characteristics of 0.55 vol. % GNS/TPU nanocomposites beyond 400 K are more pronounced due to the interfacial and orientation polarization. Mechanical characteristics evaluation of GNS/TPU composites shows a marked increase in the ultimate tensile strength without compromising their ductility and stiffness.

Keywords: dielectric spectroscopy, polarization, liquid exfoliation, mechanical charateristics

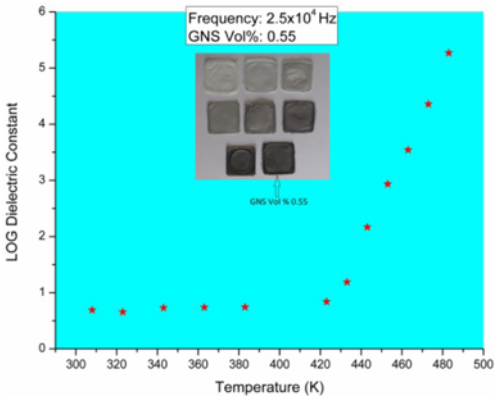

1. INTRODUCTION

In recent times, polymeric nanocomposites (PNCs), based on the conductive inclusions, are drawing considerable interest for their potential use in electronic engineering.[1] Graphene, owing to its extraordinary electrical properties, is one such conducting filler, which has been extensively studied for tuning the electrical properties of polymers.[2,3] Apart from many other applications,[4,5] graphene has been imparted to the polymers for the investigation of dielectric characteristics of nanocomposites.[6-9] Owing to the zero band gap of graphene, it is a suitable candidate for radio frequency device applications.[10] Another critical application of graphene/PNCs is energy storage for advanced technologies. The electrical energy density, ($U_e = ½\varepsilon_0\varepsilon_r E^2$), directly depends on relative permittivity ε_r and electric field.[11] For PNCs, the dielectric constant can be increased by adding ceramic fillers to it.[12] However, a high ceramic filler loading (beyond 50% vol) is required to considerably increase the dielectric constant.[13] Also, with the increase of filler loading, the mechanical characteristics of the nanocomposites suffer a decline. The last few years have seen a revival in the study of polymers reinforced by two-dimensional fillers, especially graphene due to its exceptionally high modulus (Y ≈ 1 TPa) and strength (σ_B ≈ 130 GPa).[14] It has been notably shown that graphene is employed to provide reinforcement at close to the theoretical maximum.[15] Graphene, with its zero band gap structure, possesses high carrier mobility at room temperature (≈10 000 $cm^2\ V^{-1}\ s^{-1}$) and a large theoretical specific surface area (2630 $m^2\ g^{-1}$). These mechanical and electrical characteristics of graphene make it an ideal choice for enhancement of such properties in PNCs.[16] Graphene has been added to various polymers and reported for a low percolation threshold in most of these polymers.[17] Recently, we have studied a very low percolation threshold (0.55%vol GNS) for graphene nanosheets (GNS) dispersed in thermoplastic polyurethane (TPU) nanocomposites to be published elsewhere. The formation of conducting network in nanocomposites at such low volume fractions is attributed to various reasons like: (1) large surface-to-volume ratio, (2) morphology, (3) dimensions, and (4) dispersion of

*Corresponding author: rahimjan@scme.nust.edu.pk

the nano inclusions. All these factors add up to form a large interaction zone inside the nanocomposite, which ultimately plays a vital role in the final outcome of the dielectric properties.[18] In this work, we have used GNS/TPU (up to 0.55%vol GNS) system for the dielectric spectroscopic evaluation both at room and high temperatures. Mechanical characteristics of the above-mentioned composites have also been evaluated. The enhancement in the tensile strength of nanocomposites at very low GNS loading is very adequate. Dielectric spectroscopy is a simple technique for precise measurements of electrical properties. Dielectric constant, dielectric loss, and AC conductivity are the main parameters discussed here for 0 - 0.55% vol samples at room temperature. Dielectric spectroscopy for 0.55%vol GNS sample at elevated temperatures (up to 473 K) is also reported. Like other metallic inclusions in PNCs, the dielectric loss for graphene is also on the higher side. New efforts in this direction to use graphene for high dielectric constant and low losses have already been reported.[11] However, this seeming limitation can be utilized for application where energy dissipation is the premium requirement. We believe that the work carried out here is very promising due to its simple treatment supported by excellent results, both mechanically and electrically. The liquid-exfoliated GNS with a high aspect ratio and very good dispersion is the main factor causing huge increase in the dielectric characteristics of GNS/TPU nanocomposites at elevated temperatures along with subsequent enhancement in the tensile strength at room temperature. These properties can be utilized directly for energy dissipation and for energy storage with a slight modification.

2. EXPERIMENTAL PROCEDURE

Graphite powder supplied by Branwell graphite limited, grade RFL 99.5, is used for the liquid exfoliation process. This process is known to yield good-quality graphene.[19] N-methyl-pyrrolidone (NMP) is utilized as a solvent for the above-mentioned process with a flat-head probe sonic tip. The sonication is run for 48 hr, followed by centrifugation and filtration. Varying centrifugation rates (500, 300 rpm) are used to remove un-exfoliated graphite and size selection of GNS.[14,20-22] The filtered material, after being washed with tetrahydrofuran (THF), is placed in an oven at 60°C for drying. This dried GNS powder is re-dispersed by mild bath sonication in THF at a concentration 2 mg/mL to give stock dispersions. TPU is then dissolved in THF (concentration of 50 mg/mL) by overnight stirring, which is used for composite formation with the varying volume of GNS dispersion (GNS/THF, 2 mg/mL). Each composite dispersion is sonicated for 4 hr in a sonic bath (Branson 1510E-MT sonic bath), followed by drop casting into Teflon trays. The composites are dried at 30°C for 24 hr followed by another period at 70°C for 80 hr.

3. RESULTS AND DISCUSSION

3.1 Evaluation of the dimensions of GNS

For the evaluation of exfoliation condition and dimension measurements of the dispersed GNS, transmission electron microscope (TEM) is used. Holey carbon grids with a 400 mesh are used for the dispersed GNS drops and analyzed using a Jeol 2100 TEM at 200 kV. Figure 1 is the representative of many TEM images used for the quantitative analysis of GNS exfoliation state and dimensions. As seen in Fig. 1, we have been able to get few-layer GNS with the liquid exfoliation process. The liquid exfoliation process also facilitates getting dispersions with large quantities of GNS.[19,23] It requires a tedious assessment of the edges of each flake present in the TEM images to estimate the number of layers per nanosheet, N. The approximate TEM analyses provide the information that GNS is 1 - 10 monolayers thick with mean values around N~4. The simplest estimation of TEM analysis is the measurement of long dimensions of the GNS, which is the mean nanosheet length, L. The data for length distribution of >150 nanosheets are presented asa histogram in Fig. 1 (bottom) showing that the mean nanosheet length in this case is approximately 1.4 μm.

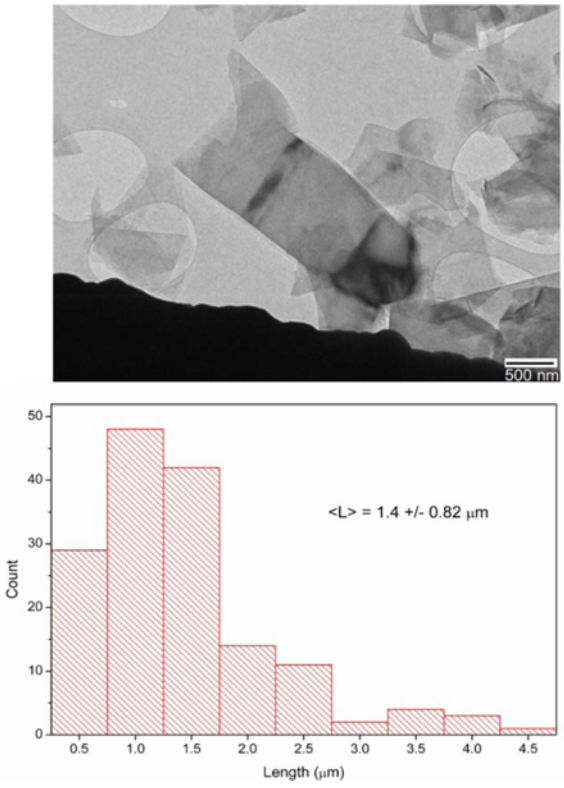

Fig. 1. Transmission electron microscopy characterization of exfoliated, size-selected GNS. The image on the top is the representative TEM image, while the bottom image is a histogram derived by measuring the lengths of >150 nanosheets from the TEM images.

3.2 Dielectric spectroscopy

The main premises of our work lie in the exfoliation of graphite crystallites by liquid exfoliation to achieve few-layer GNS and their use in TPU for tuning the dielectric properties. Generally, the electrical and mechanical properties of the nanocomposites are vigorously driven by the size of the filler.[15,20] In this work, we have acquired large aspect ratio GNS by utilizing centrifugation technique[24] and dispersing them homogeneously in the TPU matrix. Dielectric characteristics of the GNS/TPU composites (free-standing films) are obtained by using a precision impedance analyzer (Wayne Kerr 6500B). The applied alternating electric field, across the sample (8 mm diameter and 50 micron thickness), is 10 mV with frequency ranging from 100 Hz to 5 MHz. The sample holder consists of two copper rods, with smoothly finished surfaces (8 mm diameter), which are arranged in parallel plates capacitor configuration. Capacitance and dielectric tangent loss were observed directly, while dielectric constant, dielectric loss, and AC conductivity were derived as under.[25] The complex permittivity is represented as

$$\varepsilon = \varepsilon' - i\varepsilon'' \tag{1}$$

where the real part ε' gives the dielectric constant and the imaginary part depicts the dielectric loss. Dielectric constant, a quantity measuring the ability of a substance to store electrical energy in an electric field, can be calculated by using the following equation

$$\varepsilon' = \frac{Cd}{A\varepsilon_0} \tag{2}$$

where C is the observed capacitance of the sample, d is the thickness, A is the area, and ε_0 is the permittivity of free space. Dielectric loss can be calculated from dielectric tangent loss, which is observed directly from the instrument

$$\tan\delta = \frac{\varepsilon''}{\varepsilon'} \tag{3}$$

Tangent loss is the dissipation factor D, which is a measure of the energy dissipated by a dielectric material when in an oscillating field. There can be various mechanisms for the energy dissipation inside the nanocomposites, like interfacial polarization loss, dipolar polarization loss, and conduction loss. The AC conductivity for the dielectric nanocomposites here is calculated using the following equation:

$$\sigma_{AC} = \omega\varepsilon_0\varepsilon'\tan\delta \tag{4}$$

All the above-mentioned parameters are obtained as a function of frequency at room temperature in the first case for all the GNS concentrations. For the 0.55%vol GNS composite, the temperature is increased from room temperature to 473 K, and the above-mentioned parameters are calculated. Another important parameter, electric modulus, is also considered at this stage given as under.[26]

$$M = \frac{1}{\varepsilon} \tag{5}$$

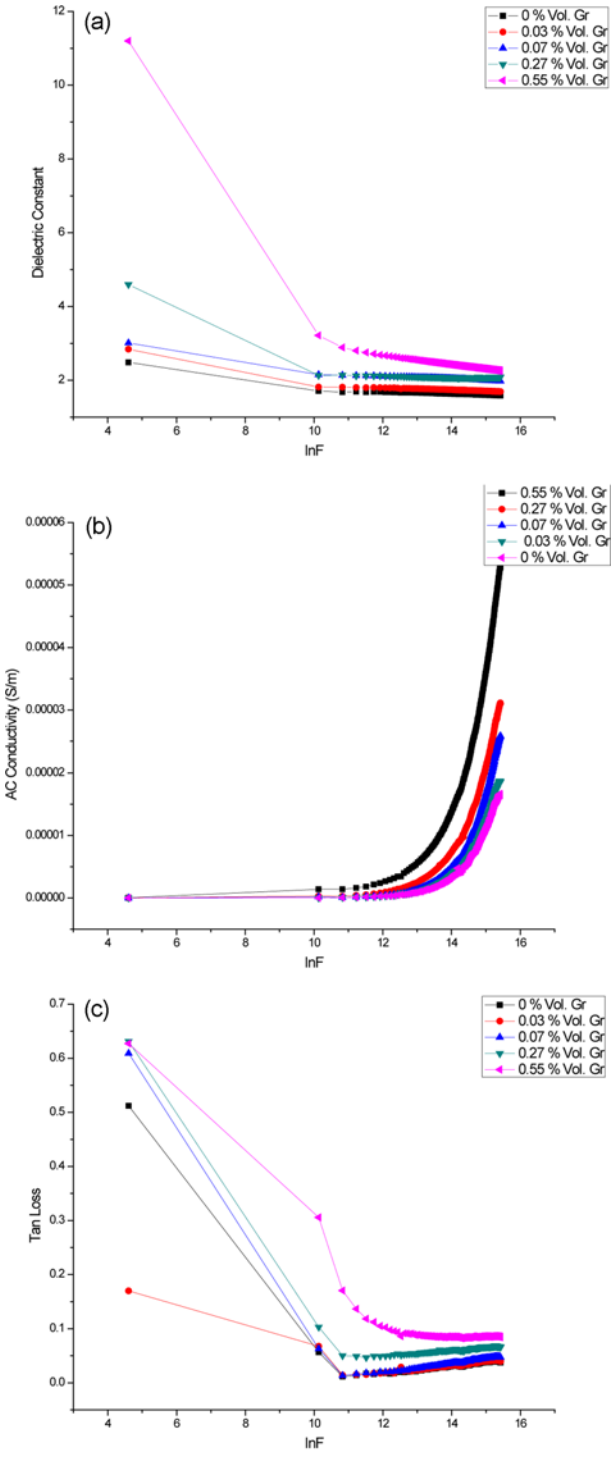

Fig. 2. Dielectric characteristics response at room temperature: (a) Dielectric constant, (b) AC conductivity, and (c) dielectric tangent loss of TPU-GNS nanocomposite as a function of frequency. The GNS loading range is (0 - 0.55)% volume.

$$M = M' + iM'' \quad (6)$$

Both the real part (M') and the imaginary part (M'') of electric modulus (M) can be evaluated as

$$M' = \frac{\varepsilon'}{\varepsilon'^2 + \varepsilon''^2} \quad (7)$$

$$M'' = \frac{\varepsilon''}{\varepsilon'^2 + \varepsilon''^2} \quad (8)$$

3.2.1 Various Loaded GNS/TPU Composites at Room Temperature

Figure 2 shows the variation of various parameters (dielectric constant, dielectric tangent loss, and AC conductivity) for different GNS loadings in TPU as a function of frequency at room temperature. As clearly shown in Fig. 2(a), the dielectric constant of the GNS/TPU composites remains almost constant through the whole frequency range with an observable increase for the maximum loading at lower frequency region. This increase in the dielectric constant for 0.55% vol GNS at lower frequencies is credited to the Maxwell-Wagnar-Sillars interfacial polarization, as there is a marked difference in the conductivity of the filler GNS and the host TPU.[17] Figure 2(b) shows the AC conductivity response of GNS/TPU composites as a function of frequency. It clearly confirms the linear relationship between these two parameters. In the low frequency range, AC conductivity for all the vol. % GNS concentrations has a steady behavior due to the charge accumulation at the interface region of the samples and electrode. This behavior transforms to a sort of exponential increase in the conductivity at higher frequencies after a certain volume fraction.[2] This is a typical behavior for disordered solids and is believed to happen due to the charge transport via hopping.[2,17] For dielectric tangent loss (Fig. 2(c)), the experimental data depict an initial decrease at lower frequency region and increase when the frequency ascends. The reason for the lower frequency region behavior can be explained with respect to percolation effect primarily occurring due to direct current conduction. There is a minor increase in the dielectric tangent loss at higher frequencies.[17] It is clear from this data that gradual addition of only a very small amount of GNS results in the continual increase of the dielectric constant, AC conductivity, and dielectric tangent loss.

3.2.2 Highest-loaded GNS/TPU Composite at Elevated Temperatures

The dielectric characteristics for the highest-loaded GNS/TPU composites (0.55% vol GNS) as a function of frequency at various temperatures are studied in this section.

3.2.2.1 Dielectric Constant and Dielectric Tangent Loss

Figure 3 shows the experimental data for dielectric constant and dielectric tangent loss in a temperature range of 308 - 473 K in two different portions. Dielectric constant and

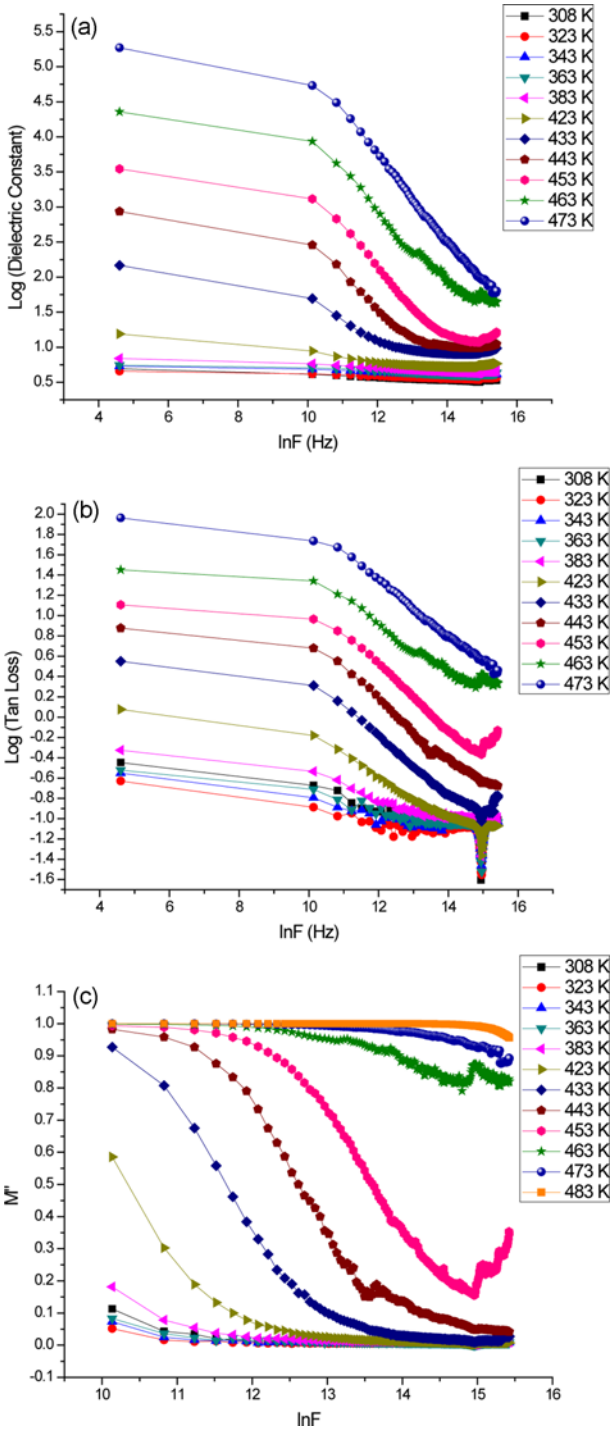

Fig. 3. (a) Dielectric constant, (b) dielectric tangent loss, and (c) electric modulus behavior of the highest loaded GNS (0.55% vol GNS)/TPU nanocompositeat various temperatures (308 - 473 K).

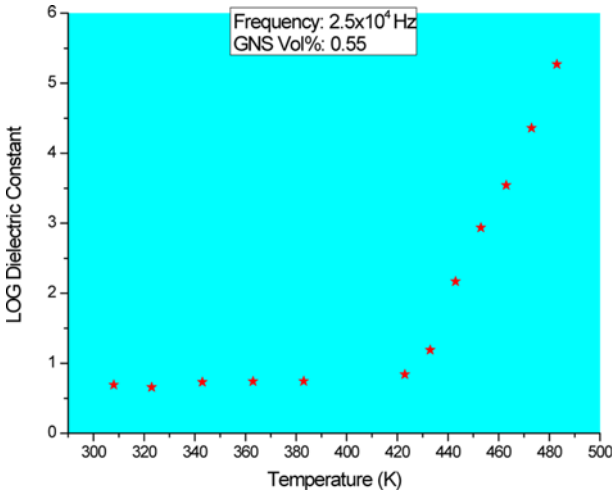

Fig. 4. Dielectric constant enhancement for GNS vol. % 0.55 as a function of temperature at 2.5 × 10^4 Hz.

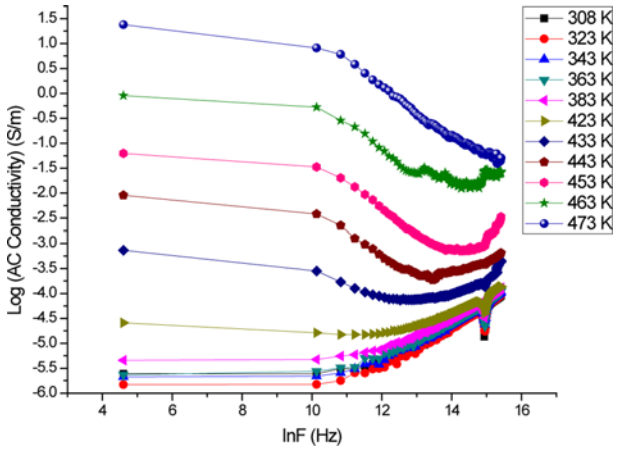

Fig. 5. AC conductivity presentation of the highest-loaded GNS (0.55% vol GNS)-TPU nanocomposite at various temperatures (308 - 473 K) as a function of frequency.

tangent loss behavior of the nanocomposite up to 383 K remain the same at room temperature. There appears a sudden increase for both dielectric constant and dielectric tangent loss behavior at lower frequency regions when the temperature is increased from 383 K to 423 K as shown in Fig. 3(a-b). The trend for both the dielectric parameters under discussion is that the two increase with increasing temperature. The room temperature values for dielectric constant and dielectric tangent loss at 25 kHz are around 11 and 0.6, respectively. At 473 K (25 kHz), dielectric constant increases to ~5 × 10^5, and dielectric tangent loss value is found to be ~107. This huge increase in both the parameters at elevated temperatures is found to be due to the electrode polarization effect, whereas electric modulus formalism led to removal of the electrode polarization effect at low frequencies.[12] The electric modulus imaginary part (M'') is shown in Fig. 3(c) from which it is evident that the relaxation peak shifts towards increasing frequencies with the increase in temperature. This shift in the peak is recognized as interfacial polarization also termed as Maxwell-Wagner-Sillars polarization.[9] The enhancement in dielectric constant as a function of temperature for 0.55% vol GNS/TPU nanocomposite at 2.5 × 10^4 Hz frequency is shown in Fig. 4.

3.2.2.2 AC Conductivity

As mentioned in the preceding section, increase in AC conductivity for GNS/TPU composites is caused by the hopping mechanism. The hopping conduction is based on both the frequency and temperature parameters. Here, the experimental effect of both these parameters for GNS/TPU composite is discussed. The AC conductivity response of the 0.55% vol GNS/TPU composite is shown in Fig. 5 as a function of frequency at various temperatures. There are two distinct phenomena occurring: one up to 423 K temperature and the other above this temperature (Fig. 5). For AC conductivity at lower temperatures, the following relationship is followed:[27]

$$\sigma_{AC}(\omega) = A\,\omega^{s} \tag{9}$$

Which means that AC conductivity is mainly dependent on the frequency and marginally changes with temperature up to 423 K. A is the proportionality constant, and s is the exponential factor ranging between 0.7 and 0.9 at lower temperatures, which vanishes at high temperatures. In the present scenario, AC conductivity remains almost constant at lower frequencies (termed as DC conductivity plateau) and increases exponentially at higher frequencies. The interfacial polarization effect is responsible for this kind of behavior because at lower frequencies the dipoles induced inside get enough time (relaxation phenomena) to orient themselves along the direction of the field while at high frequencies, due to less relaxation time, it is very difficult for the dipoles to reorient themselves. At higher frequencies, charge carriers due to the excitations hop around the nearby conductive sites back and forth causing an increase in the effective conductivity.[25] At high temperatures, the AC conductivity behavior is distinctive. It can be explained via activation energy equation.[27] Due to higher mobility of the charge carriers at lower frequencies, there appears an exceedingly high DC conductivity plateau. The AC conductivity approaches the DC conductivity values for lower frequencies and high temperatures.

$$\sigma_{AC} = A\exp\left(-\frac{E}{kT}\right) \tag{10}$$

Figure 5 clearly follows the above-mentioned equation at high temperatures and shows the maximum-achieved AC conductivity for the highest-loaded GNS/TPU composite at

473 K. Beyond this temperature, the polymer decomposes as the thermal decomposition for the TPU used in this case begins at around 500 K.

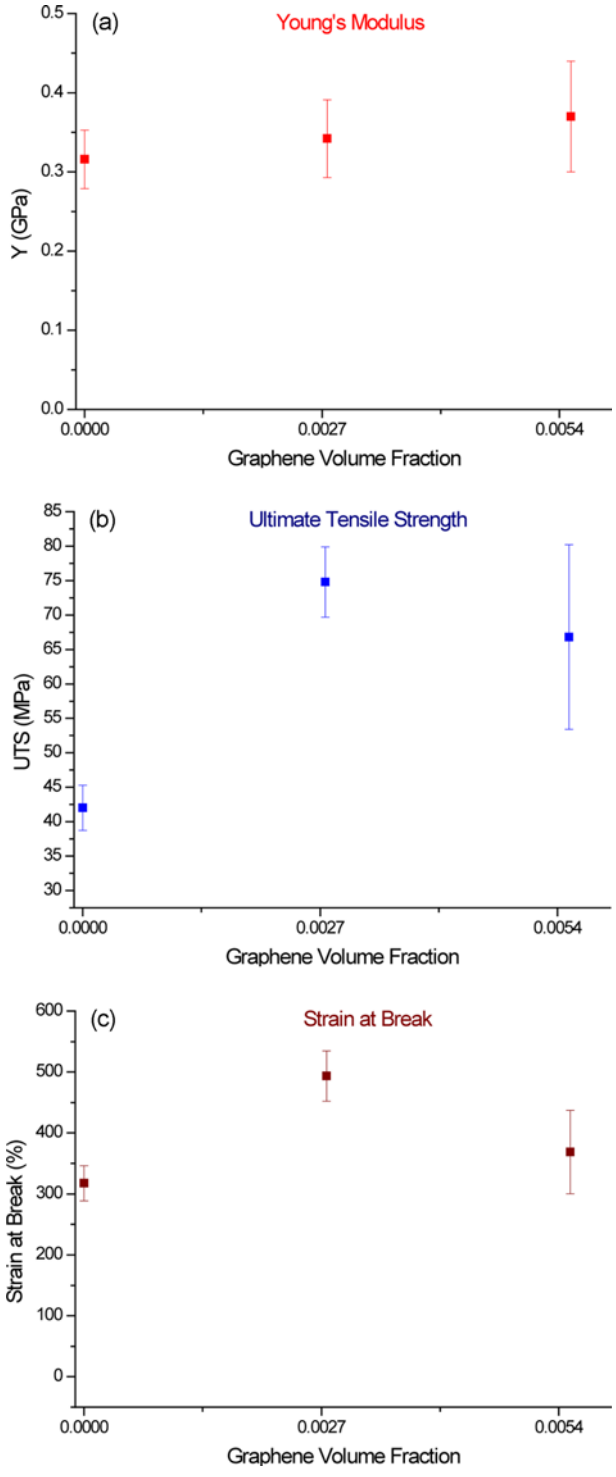

Fig. 6. (a) Young's modulus, (b) ultimate tensile strength, and (c) strain at break of GNS/TPU composites plotted as a function of GNS volume fraction.

3.3 Mechanical characteristics

The mechanical characteristics of any material are of great importance in terms of the applications, as they give a fair idea of the robustness of the material under discussion. Few of the above-mentioned GNS/TPU nanocomposites are tested mechanically in tensile testing mode. Three different specimens with respect to the volume fraction are considered here; pure polymer (TPU), 0.27 and 0.55 vol. % GNS. At least five samples for each specimen are tested mechanically, as the samples are cut into strips of width 2.25 mm, and mechanical testing is performed using Zwick Roell Tensile tester with a 100 N load cell at a strain rate of 50 mm/min. Three parameters, Young's modulus, ultimate tensile strength, and strain at break, are analyzed to give information on the mechanical robustness of the nanocomposites. A marked increase in the ultimate tensile strength is observed for all the samples (assumingly). For the pure polymer (TPU), the UTS is around 40 MPa, which is increased to 65 - 75 MPa for the GNS-filled nanocomposites with the maximum increase for the 0.27 vol. % GNS (Fig. 6(a)). Although the stiffness (Young's modulus) remains unchanged with a slight increase for the nanocomposites up to 0.55 vol. % GNS, the strain at break is increased as shown in Fig. 6(b-c). These mechanical characteristics add to the already described dielectric spectroscopic results, making the GNS/TPU nanocomposites: a potential candidate for future electronic engineering applications.

4. CONCLUSIONS

The composites of graphene nanosheets (high aspect ratio) and thermoplastic polyurethane are prepared here with a very simple one-step formation method, drop casting. At room temperature, the dielectric constant, AC conductivity, and dielectric tangent loss experience considerable increase for 0.55% vol. The dielectric constant and tangent loss for TPU are around ~2 and ~0.03, respectively. For 0.55% vol GNS/TPU nanocomposite, dielectric constant and AC conductivity are increased six times at 100 Hz and 10 -1000 times with respect to the pristine TPU, respectively, over a whole frequency range. This sample is then tested for the same properties at increasing temperature, and very encouraging results are revealed with extremely high dielectric constant (5×10^5 at 25 kHz and 473 K), good AC conductivity (~25 S/cm at 25 kHz and 473 K), and very high dielectric tangent loss (~95 at 25 kHz and 473 K). Interfacial and orientation polarization effects are the main causes behind the enhancement in the dielectric properties of the GNS/TPU nanocomposites. The mechanical properties are considerably enhanced, especially the ultimate tensile strength that is almost doubled with a minor increment in GNS loading. The stiffness and ductility of the nanocomposites are not compromised with the GNS loading. These free-standing

composite films are conductive, flexible, and very easy to process. We believe that the dielectric spectroscopy of the GNS/TPU with high GNS concentrations around 30 - 50 wt. % will provide more productive results for the related applications like strain sensors, energy dissipation, and many other related fields.

ACKNOWLEDGEMENTS

We acknowledge the guidance and support from Dr. Umar Khan and Prof. Jonathan N. Coleman, School of Physics, CRANN and AMBER, Trinity College Dublin, Ireland.

REFERENCES

1. A. Dimiev, D. Zakhidov, B. Genorio, K. Oladimeji, B. Crowgey, L. Kempel, E. J. Rothwell, and J. M. Tour, *ACS Appl. Mater. Interfaces* **5**, 7567 (2013).
2. I. Tantis, G. C. Psarras, and D. Tasis, *Express Polym. Lett*. **6**, 283 (2012).
3. R. Balasubramaniyan, V. H. Pham, J. Jang, S. H. Hur, and J. S. Chung, *Electron. Mater. Lett*. **9**, 837 (2013).
4. Y. Zhao, Y. Huang, Q. Wang, X.Y. Wang, M. Zong, H. Wu, and W. Zhang, *Electron. Mater. Lett*. **9**, 683 (2013).
5. A. J. Akhtar, A. Gupta, B. K. Shaw, and S. K. Saha, *Appl. Phys. Lett.* **103**, 242902 (2013).
6. J. Syurik, O. A. Ageev, B. G. Konoplev, D. I. Cherednichenko, and A. Axeev, *Carbon* **63**, 317 (2013).
7. P. Barber, S. Balasubramanian, Y. Anguchamy, S. Gong, A. Wibowo, H. Gao, H. J. Ploehn, and H. C. Loye, *Materials* **2**, 1697 (2009).
8. H. Kim, Y. Miura, and C. W. Macosko, *Chem. Materials* **22**, 3441 (2010).
9. I. Tantis, G. C. Psarras, and D. Tasis, *Express Polym. Lett*. **6**, 283 (2012).
10. L. Liao and X. F. Duan, *Mater Sci. Eng. R Rep*. **70**, 354 (2010).
11. J. Shang, Y. Zhang, L. Yu, B. Shen, X. Luan, F. Lv, and P. K. Chu, *J. Mater. Chem. A* **1**, 884 (2013).
12. X. Huang, C. Zhi, P. Jiang, D. Golberg, Y. Bando, and T. Tanaka, *Nanotechnology* **23**, 455705 (2012).
13. K. Yu, H. Wang, Y. Zhou, Y. Bai, and Y. Niu, *J. Appl. Phys.* **113**, 034105 (2013).
14. R. Jan, P. May, A. P. Bell, A. Habib, U. Khan, and J. N. Coleman, *Nanoscale* **6**, 4889 (2014).
15. P. May, U. Khan, A. O'Neill, and J. N. Coleman, *J. Mater. Chem.* **22**, 1278 (2012).
16. X. Huang, X. Qi, F. Boey, and H. Zhang, *Chem. Soc. Rev.* **41**, 666 (2011).
17. J. Shang, Y. Zhang, L. Yu, B. Shen, F. Lv, and P. K. Chu, *Mater. Chem. Phys.* **134**, 867 (2012).
18. M. Roy, J. K. Nelson, R. K. MacCrone, L. S. Schadler, C. W. Reed, R. Keefe, and W. Zenger, *IEEE T Dielect. El. In.* **12**, 629 (2005).
19. J. N. Coleman, M. Lotya, A. O'Neill, S. D. Bergin, P. J. King, U. Khan, K. Young, A. Gaucher, S. De, R. J. Smith, I. V. Shvets, S. K. Arora, G. Stanton, H. Y. Kim, K. Lee, G. T. Kim, G. S. Duesberg, T. Hallam, J. J. Boland, J. J. Wang, J. F. Donegan, J. C. Grunlan, G. Moriarty, A. Shmeliov, R. J. Nicholls, J. M. Perkins, E. M. Grieveson, K. Theuwissen, D. W. McComb, P. D. Nellist, and V. Nicolosi, *Science* **331**, 568 (2011).
20. U. Khan, A. O'Neill, H. Porwal, P. May, K. Nawaz, and J. N. Coleman, *Carbon* **50**, 470 (2012).
21. M. Lotya, P. J. King, U. Khan, S. De, and J. N. Coleman, *ACS Nano* **4**, 3155 (2010).
22. A. O'Neill, U. Khan, and J. N. Coleman, *Chem. Mater.* **24**, 2414 (2012).
23. P. May, U. Khan, J. M. Hughes, and J. N. Coleman, *J. Phys. Chem. C* **116**, 11393 (2012).
24. G. E. Padawer and N. Beecher, *Polym. Eng. Sci.* **10**, 185 (1970).
25. S. Maiti, N. K. Shrivastava, S. Suin, and B. B. Khatua, *Express Polym. Lett*. **7**, 505 (2013).
26. J. Belattar, M. P. F. Graça, L. C. Costa, M. E. Achour, and C. Brosseau, *J. Appl. Phys.* **107**, 124111 (2010).
27. A. Osak, *Ferroelectrics* **418**, 52 (2011).